Hindawi
Discrete Dynamics in Nature and Society
Volume 2020, Article ID 9279315, 9 pages
https://doi.org/10.1155/2020/9279315

Research Article

Stability Analysis of Regular and Chaotic Ca^{2+} Oscillations in Astrocytes

Min Ye[1] and Hongkun Zuo[2]

[1]*School of Education Science, Guangxi University for Nationalities, Nanning 530006, Guangxi, China*
[2]*School of Finance and Mathematics, Huainan Normal University, Huainan 232038, Anhui, China*

Correspondence should be addressed to Hongkun Zuo; hk_zuo@163.com

Received 13 July 2020; Revised 5 September 2020; Accepted 12 September 2020; Published 23 September 2020

Academic Editor: Jia-Bao Liu

Ca^{2+} oscillations play an important role in various cell types. Thus, understanding the dynamical mechanisms underlying astrocytic Ca^{2+} oscillations is of great importance. The main purpose of this article was to investigate dynamical behaviors and bifurcation mechanisms associated with astrocytic Ca^{2+} oscillations, including stability of equilibrium and classification of different dynamical activities including regular and chaotic Ca^{2+} oscillations. Computation results show that part of the reason for the appearance and disappearance of spontaneous astrocytic Ca^{2+} oscillations is that they embody the subcritical Hopf and the supercritical Hopf bifurcation points. In more details, we theoretically analyze the stability of the equilibrium points and illustrate the regular and chaotic spontaneous calcium firing activities in the astrocytes model, which are qualitatively similar to actual biological experiment. Then, we investigate the effectiveness and the accuracy of our nonlinear dynamical mechanism analysis via computer simulations. These results suggest the important role of spontaneous Ca^{2+} oscillations in conjunction with the adjacent neuronal input that may help correlate the connection of both the glia and neuron.

1. Introduction

There are two types of cells (namely, the neuron and the glia) in the central nervous system (CNS). Neuron is the basic structural and functional elements of the CNS and has the function of contacting and integrating input information and transmitting information [1, 2]. With the aid of electron microscope, it was found that the neuron is divided into two parts: the cell body and the protrusion. The role of the protrusion is to receive the impulse from the axon of other neurons and transfer to the cell body. Unlike the neuron, as another type of cell, the glia also has the protrusion, but without the dendrites or the axons. It is demonstrated that the glia, of which ratio of the amount to neuron is about 10 : 1, is widely distributed in the CNS. The glia includes astrocyte, oligodendrocyte (combined with the astrocyte as macroglia), and microglia. In the past decades, the role of astrocytes in the CNS has been recognized that the transmission and integration of information is performed by network of neurons. The glia is the only passive auxiliary role, supporting, providing nutrition, and assisting metabolism [3, 4]. In recent years, lots of studies have attempted to show that the glia has great potential to provide new insight into other roles (assisting the functional activities of neuron) besides having an effect on supporting and isolating the neighboring neurons [5]. The evidences that indicate that the glia cooperates with the neuron come from a large number of experiments by Newman and Zahs [6]. As the second messenger, calcium oscillation is referred to cytoplasmic calcium ions as transducing information in a manner of concentration oscillation, which affects various processes such as cell differentiation, maturation, and apoptosis. One of the earliest reactions produced by all cells after physiological stimulation is of an increase in the concentration of calcium ions in the cytoplasm [1]. The astrocyte located near synapse of neighboring neuron responds to glutamate, ATP, etc., with evaluation of calcium oscillations. Excitatory glutamate released by neuron can activate not only the neighboring neuron but also glutamate receptor of astrocyte increasing the calcium ion concentration [7]. It is shown that calcium oscillation is not only the basic way of astrocyte excitement but also the basic mode of biological information exchange between the neuron and

astrocyte [8, 9]. In contrast with the neuron, astrocyte generates neuronal-dependent and spontaneous calcium oscillation, which is similar to the glutamate-dependent calcium waves, releasing glutamate affected by the neuron [10].

In the last decades, based on biological background of calcium oscillation in the neuron and astrocyte, a wide variety of mathematical models are constructed to investigate in detail the stability and dynamical mechanism of calcium activities in the neuron and astrocyte [11–15]. It has long been appreciated that the location of the bifurcations is of great interest in many dynamical systems and it has emerged as a major component in the analysis of mathematical models. It is well known that there are three traditional software packages (Matlab and AUTO) that are used to solve the continuation and the bifurcation of mathematical models [16, 17]. Therefore, flexible, yet computable, and dynamical analysis of calcium oscillations (separately, firing, bursting, quasi-periodic, and chaotic activity), as well as waves involved in the biological process in the CNS is required. Regular oscillatory activity is classified into firing and bursting, which is based on the dynamics of fast and slow systems [18]. For quasiperiodic and chaotic activity, it refers to seemingly random irregular motion that occurs in a deterministic system described by deterministic theory with uncertainty and unpredictability. In a large number of the free calcium oscillation experiments of the neuron and astrocyte, it was found that bursting is of an important role in information transmission [19–23].

There is strong experimental evidence for bidirectional information communication between the glia and neuron in biological signaling pathway [22]. As the major neurotransmitter, glutamate released from the neuron may have an autonomous effect on the adjacent glia by the intracellular calcium oscillations. Trying to recognize the dynamical mechanism of different phenomena of calcium oscillatory activities, based on the bidirectional signaling pathway between the neuron and glia of the CNS in different brain regions, critical and constructive analysis of existing published review literatures are provided both from experimental and theoretical point of view [24–26]. The establishment of the first dynamic model describing the process of generating neuronal firing activities began with a series of work by Hodgkin and Huxley in the 1950s. Based on the bioelectric theory and giant axon experiment, they successfully established a mathematical neuron model for the first time through a series of nonlinear differential equations that reproduce different oscillatory patterns of neuron observed in the experiment. On this neurophysiological basis of their finds, many other mathematical models associated with cell membrane ion channels were established with purpose of describing rich firing oscillations of different types of neurons in the experiment [27]. Although these neuron models are the mathematical reduction of the HH model, they can simulate the experimental phenomena from a wide variety of cell types and thus have been extensively studied [28].

In order to understand the dynamical mechanisms involved in spontaneous Ca^{2+} oscillations in the astrocyte, Lavrentovich and Hemkin proposed a dynamical model of how the different types of Ca^{2+} oscillations occur in real astrocyte in the CNS [29]. Spontaneous Ca^{2+} oscillations have been extensively observed in the cytosol of the glia both in situ and in vivo originating in the hippocampus and thalamus of the brain [30]. Although the functional and structural perspective of spontaneous behaviors is not yet well understood, many physiological experimental results indicate that, in conjunction with outer input, spontaneous Ca^{2+} oscillations may help correlate the connection between the glia and neuron. It is known that different types of these oscillatory activities in astrocytes vary with bifurcation principles, stability analysis, and simulations that underlie activation and inhibition of regular and chaotic Ca^{2+} oscillations which should be discussed in detail both from theoretical and experimental point of view.

2. Model Description

In this study, we analyze a two-compartment astrocyte model proposed by Lavrentovich and Hemkin as an example of a system that exhibits regular and chaotic calcium oscillations. This model involves currents such as the free calcium concentration (Ca_{cyt}) in cytosol and in ER (Ca_{er}), and IP_3 concentration as intracellular messenger in astrocyte (IP_3). V_{CICR} and V_{serca} denote calcium flux from ER to cytosol and sarcoplasmic reticulum ATPase that reach ER from cytosol, respectively [31–34]. The model can be described as follows:

$$\begin{cases} \dfrac{d\mathbf{Ca}_{\mathbf{cyt}}}{\mathbf{dt}} = \mathbf{v}_{\mathbf{in}} + \mathbf{V}_{\mathbf{CICR}} - 0.5\mathbf{Ca}_{\mathbf{cyt}} - \mathbf{v}_{\mathbf{M2}}\left(\dfrac{\mathbf{Ca}_{\mathbf{cyt}}^2}{\mathbf{Ca}_{\mathbf{cyt}}^2 + 10^{-2}}\right) + 0.5\left(\mathbf{Ca}_{\mathbf{er}} - \mathbf{Ca}_{\mathbf{cyt}}\right), \\ \dfrac{d\mathbf{Ca}_{\mathbf{er}}}{\mathbf{dt}} = \mathbf{v}_{\mathbf{M2}}\left(\dfrac{\mathbf{Ca}_{\mathbf{cyt}}^2}{\mathbf{Ca}_{\mathbf{cyt}}^2 + \mathbf{k}_2^2}\right) - \mathbf{k}_{\mathbf{f}}\left(\mathbf{Ca}_{\mathbf{er}} - \mathbf{Ca}_{\mathbf{cyt}}\right) - \mathbf{V}_{\mathbf{CICR}}, \\ \dfrac{d\mathbf{IP}_3}{\mathbf{dt}} = 0.05\left(\dfrac{\mathbf{Ca}_{\mathbf{cyt}}^2}{\mathbf{Ca}_{\mathbf{cyt}}^2 + \mathbf{k}_{\mathbf{p}}^2}\right) - 0.08\,\mathbf{IP}_3, \end{cases} \tag{1}$$

where

$$\mathbf{V}_{\mathrm{CICR}} = 4\left(\mathbf{Ca}_{\mathbf{er}} - \mathbf{Ca}_{\mathbf{cyt}}\right)\mathbf{v}_{\mathrm{M3}}\left(\frac{0.27^{\mathbf{n}}\mathbf{Ca}_{\mathbf{cyt}}^{\mathbf{n}}}{\left(\mathbf{Ca}_{\mathbf{cyt}}^{\mathbf{n}} + 0.27^{\mathbf{n}}\right)\left(\mathbf{Ca}_{\mathbf{cyt}}^{\mathbf{n}} + \mathbf{k}_{\mathbf{CaI}}^{\mathbf{n}}\right)}\right) \times \left(\frac{\mathbf{IP}_3^{\mathbf{m}}}{\mathbf{IP}_3^{\mathbf{m}} + \mathbf{k}_{\mathbf{ip3}}^{\mathbf{m}}}\right). \tag{2}$$

Since the parameter v_{in} is calcium ion flux from outer extracellular space through membrane of the astrocyte and into the cytosol, in this work, we choose v_{in} to be the bifurcation parameter to control the spontaneous calcium oscillatory activities. The other physiological parameter values are $v_{M3} = 40\ \mathrm{s}^{-1}$, $k_{CaI} = 0.27\ \mu\mathrm{M\ s}^{-1}$, $k_{\mathrm{ip3}} = 0.1\ \mu\mathrm{M\ s}^{-1}$, $v_{M2} = 15\ \mu\mathrm{M\ s}^{-1}$, $k_2 = 0.1\ \mu\mathrm{M}$, $k_f = 0.5\ \mu\mathrm{M\ s}^{-1}$, and $k_p = 0.164\ \mu\mathrm{M}$.

3. Stability Analysis and Bifurcation of Equilibrium

Let $x = (x, y, z)^{\mathrm{T}} = (Ca_{\mathrm{cyt}}, Ca_{\mathrm{er}}, IP_3)^{\mathrm{T}}$, $r = v_{\mathrm{in}}$, system (1) can be rewritten as

$$\begin{cases} \dot{x} = \dfrac{1}{2}\mathbf{y} + (\mathbf{r} - \mathbf{x}) - 15 \quad \mathbf{d}1 - 11.4\mathbf{x}^{\mathbf{n}}\mathbf{d}2\mathbf{z}^{\mathbf{m}}\mathbf{d}3, \\ \dot{y} = \dfrac{1}{2}(\mathbf{x} - \mathbf{y}) + 15 \quad \mathbf{d}1 + 11.4\mathbf{x}^{\mathbf{n}}\mathbf{d}2\mathbf{z}^{\mathbf{m}}\mathbf{d}3, \\ \dot{z} = 10^{-2}\left(5\mathbf{x}^2\mathbf{d}4 - 8\mathbf{z}\right), \end{cases} \tag{3}$$

where $d1 = x^2/(x^2 + 10^{-2})$, $d2 = (x\text{-}y)/(x^{\mathrm{n}} + 7 \times 10^{-2})$, $d3 = 1/(z^{\mathrm{m}} + 6 \times 10^{-3})$, and $d4 = 1/(x^2 + 27 \times 10^{-3})$.

Equilibrium of (3) takes the form

$$\begin{cases} \mathbf{x} = 2\mathbf{r}, \\ \mathbf{z} = \dfrac{5}{8}\mathbf{x}^2\mathbf{d}4, \\ \mathbf{y} = 2\left(15 \quad \mathbf{d}1 - 11.4\mathbf{x}^{2.02}\mathbf{z}^{2.2}\mathbf{d}2 \quad \mathbf{d}3 + \mathbf{r}\right). \end{cases} \tag{4}$$

Let $(x_0, y_0, z_0)^{\mathrm{T}}$ be the root of (3) and $x_1 = x - x_0$, $y_1 = y - y_0$, and $z_1 = z - z_0$, and we are able to obtain the following equations:

$$\begin{cases} \dot{x}_1 = \mathbf{r} - \mathbf{x} + \dfrac{1}{2}\left(2\mathbf{y} - \dfrac{\mathbf{p}_2\mathbf{x}^2}{\mathbf{d}2}\right) - \dfrac{\mathbf{p}_3\mathbf{x}^{2.02}\mathbf{z}^{2.2}(\mathbf{x} - \mathbf{y})}{\mathbf{d}2 \quad \mathbf{d}3}, \\ \dot{y}_1 = \dfrac{1}{2}(\mathbf{x} - \mathbf{y} + \mathbf{p}_2\mathbf{d}1) + \mathbf{p}_3\mathbf{x}^{\mathbf{n}}\mathbf{d}2\mathbf{p}_3\mathbf{d}3, \\ \dot{z}_1 = 10^{-2}\left(5\mathbf{x}^2\mathbf{d}4 - 8\mathbf{z}\right). \end{cases} \tag{5}$$

The Jacobian matrix is

$$\mathbf{A} = \left(\mathbf{a}_{\mathbf{ij}}\right)_{3\times 3}, \quad \mathbf{i}, \mathbf{j} = 1, 2, 3, \tag{6}$$

where

$$\begin{aligned} \mathbf{a}_{11} &= \mathbf{p}_2\mathbf{d}1 - \mathbf{q}_1\frac{\mathbf{p}_3 - \mathbf{p}_4\mathbf{q}_2}{\boldsymbol{\sigma}} + \mathbf{p}_5\mathbf{d}2 \quad \mathbf{d}3\frac{1}{\boldsymbol{\sigma}} - 1, \\ \mathbf{a}_{12} &= \frac{\mathbf{p}_3\mathbf{q}_1}{\boldsymbol{\sigma}} + \frac{1}{2}, \\ \mathbf{a}_{13} &= \frac{\mathbf{p}_1\mathbf{x}^{2.02}\mathbf{q}_2\mathbf{z}^{3.04}\mathbf{d}3}{\boldsymbol{\sigma}} - \frac{\mathbf{p}_1\mathbf{q}_1\mathbf{q}_2}{\boldsymbol{\sigma}\mathbf{z}}, \\ \mathbf{a}_{21} &= -\mathbf{x}\mathbf{p}_1 + \mathbf{d}1\mathbf{p}_2 + \frac{\mathbf{p}_3\mathbf{q}_1 + \mathbf{p}_4\mathbf{q}_2}{\boldsymbol{\sigma}\mathbf{x}} - \frac{\mathbf{p}_5\mathbf{x}^{3.04}\mathbf{q}_2\mathbf{q}_1\mathbf{d}1}{\boldsymbol{\sigma}} + \frac{1}{2}, \\ \mathbf{a}_{22} &= -\frac{\mathbf{p}_3\mathbf{q}_1}{\boldsymbol{\sigma}} - \frac{1}{2}, \\ \mathbf{a}_{23} &= -\frac{\mathbf{d}3\mathbf{p}_1\mathbf{x}^{2.02}\mathbf{q}_2\mathbf{z}^{3.04}}{\boldsymbol{\sigma}} + \frac{\mathbf{p}_1\mathbf{q}_1\mathbf{q}_2}{\boldsymbol{\sigma}\mathbf{z}}, \\ \mathbf{a}_{31} &= \mathbf{x} \quad \mathbf{d}1 - 10^{-1}\mathbf{x}^3\mathbf{p}_1\mathbf{q}_2, \\ \mathbf{a}_{32} &= 0, \\ \mathbf{a}_{33} &= -\frac{2}{25}, \\ \boldsymbol{\sigma} &= \frac{\mathbf{d}2}{\mathbf{d}3}, \\ \mathbf{p}_1 &= 25, \\ \mathbf{p}_2 &= 30, \\ \mathbf{p}_3 &= 11, \\ \mathbf{p}_4 &= 23, \\ \mathbf{p}_5 &= 46, \\ \mathbf{q}_1 &= \mathbf{x}^{\mathbf{n}}\mathbf{z}^{\mathbf{m}}, \\ \mathbf{q}_2 &= \mathbf{x} - \mathbf{y}. \end{aligned} \tag{7}$$

Clearly, the characteristic equation of system (5) is

$$\boldsymbol{\lambda}^3 + \mathbf{Q}_3\boldsymbol{\lambda}^2 + \mathbf{Q}_2\boldsymbol{\lambda} + \mathbf{Q}_1 = 0. \tag{8}$$

The Hurwitz matrix with the coefficients Q_i of the matrix characteristic polynomial can be rewritten as follows:

$$\begin{aligned} \mathbf{H}_1 &= (\mathbf{Q}_1), \\ \mathbf{H}_2 &= \begin{pmatrix} \mathbf{Q}_1 & 1 \\ \mathbf{Q}_3 & \mathbf{Q}_2 \end{pmatrix}. \end{aligned} \tag{9}$$

By simple computation, one can easily verify that the eigenvalues are negative or of negative real parts if the determinants of Hurwitz matrix are positive:

$$\mathbf{de}\quad \mathbf{t}(\mathbf{H_i}) > 0, \quad \mathbf{i} = 1, 2, 3. \tag{10}$$

Now, motivating the Routh–Hurwitz method, we analyze the bifurcation points of system (4) for the parameter r (that is, v_{in}):

$$\begin{aligned} \mathbf{r}_1 &= 0.0193, \\ \mathbf{r}_2 &= 0.0772. \end{aligned} \tag{11}$$

Summarizing the above stability analysis, we have linearized the model at the origin of portrait state and the following results can be described as follows:

(1) System (5) has a stable node as $0r < 0.0193$

(2) System (5) has a nonhyperbolic equilibrium $O_1 = (0.03858, 2.66776, 0.03277)$ as $r = 0.0193$

(3) System (5) has a saddle node as $0.0193r < 0.0772$

(4) System (5) has a nonhyperbolic equilibrium $O_2 = (0.15432, 0.675115, 0.29351)$ as $r = 0.0772$

(5) System (5) has a stable node as $r > 0.0772$

We denote $r = r_0$, $x_1 = x - x_0$, $y_1 = y - y_0$, $z_1 = z - z_0$, and $r_1 = r - r_0$, and the equilibrium of system (5) is (x_0, y_0, z_0). For the purpose of applying the Hopf bifurcation theory, a new variable r_1 is added to the model, where $\mathrm{d}r_1/\mathrm{d}t = 0$. The system takes the form

$$\begin{cases} \dot{x}_1 = (\mathbf{r}_1 + \mathbf{r}_0) - \mathbf{d}2 \quad \mathbf{d}3\mathbf{p}_3\mathbf{x}^{2.02}\mathbf{z}^{2.2}\mathbf{q}_2 - (\mathbf{p}_1 - 1)\mathbf{d}1 - \dfrac{1}{2}\mathbf{p}_2, \\ \dot{y}_1 = \dfrac{1}{2} + (\mathbf{p}_1 - 1)\mathbf{d}1 + \mathbf{p}_3\mathbf{q}_1\mathbf{q}_1\mathbf{d}1 \quad \mathbf{d}3, \\ \dot{z}_1 = -(\mathbf{z}_1 + \mathbf{z}_0)\dfrac{\mathbf{x}^2}{\mathbf{x}^2 + \mathbf{Q}_3}, \\ \dot{r}_1 = 0. \end{cases} \tag{12}$$

For $r_1 = 0$, the point (0, 0, 0, 0) is the equilibrium of system (12), which has the same stability as the one in (3). For $r_0 = 0.01929$, the Jacobian matrix of system (12) is

$$\begin{pmatrix} -6 \times 10 & 7 \times 10^{-1} & 4 \times 10 & 1 \\ 6 \times 10 & -7 \times 10^{-1} & -4 \times 10 & 0 \\ 10^{-1} & 0 & -8 \times 10^{-2} & 0 \\ 0 & 0 & 0 & 0 \end{pmatrix}. \tag{13}$$

Four eigenvalues of (5) are $\xi_1 = -58.0969$, $\xi_2 = 0.0225i$, $\xi_3 = -0.0225i$, and $\xi_4 = 0$, respectively. Therefore, we can have the associated eigenvector:

$$\begin{pmatrix} \mathbf{x}_* \\ \mathbf{y}_* \\ \mathbf{z}_* \\ \mathbf{r}_* \end{pmatrix} = \mathbf{U}\begin{pmatrix} \mathbf{u} \\ \mathbf{v} \\ \mathbf{w} \\ \mathbf{s} \end{pmatrix}. \tag{14}$$

Therefore, system (12) can be written as

$$\begin{pmatrix} \dot{u} \\ \dot{v} \\ \dot{w} \\ \dot{s} \end{pmatrix} = \mathbf{A}\begin{pmatrix} \mathbf{u} \\ \mathbf{v} \\ \mathbf{w} \\ \mathbf{s} \end{pmatrix} + \mathbf{S}, \tag{15}$$

where

$$\begin{aligned} \mathbf{A} &= \begin{pmatrix} -38 & 0 & 0 & 0 \\ 0 & 0 & -2 \times 10^{-2} & 0 \\ 0 & 2 \times 10^{-2} & 0 & 0 \\ 0 & 0 & 0 & 0 \end{pmatrix}, \\ \mathbf{S} &= \mathbf{U}^{-1}\begin{pmatrix} \mathbf{f}_1 \\ \mathbf{f}_2 \\ \mathbf{f}_3 \\ 0 \end{pmatrix} - \mathbf{A}\begin{pmatrix} \mathbf{u} \\ \mathbf{v} \\ \mathbf{w} \\ \mathbf{s} \end{pmatrix}. \end{aligned} \tag{16}$$

Next, we analyze the center manifold of system (12). By simple computation, we have

$$\mathbf{W}^{\mathbf{c}}_{\mathbf{loc}}(\mathbf{O}_1) = \left\{(\mathbf{u}, \mathbf{v}, \mathbf{w}, \mathbf{s})\hat{\mathbf{I}}\mathbf{R}^4 \,\middle|\, \mathbf{u} = \mathbf{h}^*(\mathbf{v}, \mathbf{w}, \mathbf{s}), \mathbf{D}\mathbf{h}^* = 0\right\}. \tag{17}$$

Substituting (17) into (15), we have

$$\begin{pmatrix} \mathbf{h}^*(\dot{\mathbf{v}}, \mathbf{w}, \mathbf{s}) \\ \dot{v} \\ \dot{w} \\ \dot{s} \end{pmatrix} = \mathbf{A}\begin{pmatrix} \mathbf{h}^*(\mathbf{v}, \mathbf{w}, \mathbf{s}) \\ \mathbf{v} \\ \mathbf{w} \\ \mathbf{s} \end{pmatrix} + \mathbf{S}. \tag{18}$$

Let $h(v, w, s) = av2 + bw2 + cs2 + dv \quad w + evs + fws + \cdots$, and the center manifold of (12) is

$$\mathbf{N}(\mathbf{h}) = 0, \tag{19}$$

where $a = 0.000567$, $b = -0.1828$, $c = -1.95096$, $d = 0.049818$, $e = -1638.5116$, and $f = -0.75265$. Then, system (12), which is confined to the manifold, is

$$\begin{pmatrix} \dot{v} \\ \dot{w} \end{pmatrix} = \mathbf{B}\begin{pmatrix} \mathbf{v} \\ \mathbf{w} \end{pmatrix} + \begin{pmatrix} \mathbf{f}^*(\mathbf{v}, \mathbf{w}) \\ \mathbf{f}^*(\mathbf{v}, \mathbf{w}) \end{pmatrix}. \tag{20}$$

Thus, we can obtain

$$\mathbf{d} = \frac{\mathbf{d}(\mathbf{Re}(\xi(\mathbf{s})))}{\mathbf{ds}}\bigg|_{\mathbf{O}_1} < 0. \tag{21}$$

Having applied the above formulas and computations, the sufficient conditions for stability can be obtained.

Conclusion 1. System (3) has a subcritical Hopf bifurcation at $r_0 = 0.01929$. If $r > r_0$, the equilibrium loses its stability, which means that a periodic solution occurs and the system oscillates.

Using the same notations above, we construct the eigenvalues of equilibrium point O_2 = (0, 0, 0, 0) as

$\xi_1 = -0.08959$, $\xi_2 = 3.3864i$, $\xi_3 = -3.3864i$, and $\xi_4 = 0$, respectively, as $r_0 = 0.07716$. On the center manifold, system (12) has the form

$$\begin{pmatrix} \dot{u} \\ \dot{v} \\ \dot{w} \\ \dot{s} \end{pmatrix} = \mathbf{U}^{-1} \begin{pmatrix} \mathbf{u} \\ \mathbf{v} \\ \mathbf{w} \\ \mathbf{s} \end{pmatrix} + \mathbf{S}, \tag{22}$$

where

$$\mathbf{S} = \mathbf{U}^{-1}\mathbf{f} - \mathbf{B} \begin{pmatrix} \mathbf{u} \\ \mathbf{v} \\ \mathbf{w} \\ \mathbf{s} \end{pmatrix}. \tag{23}$$

Note that, on the above center manifold of the system, we have

$$\mathbf{N}(\mathbf{h}) = 0. \tag{24}$$

In this case, the system confined to the center manifold is as follows:

$$\begin{aligned} \mathbf{a} &= 6 \times 10^{-1}\mathbf{f}1 + 2 \times 10^{-2}\mathbf{f}2 = -2265.4 > 0, \\ \mathbf{d} &= -7 \times 10^{-4} < 0. \end{aligned} \tag{25}$$

Based on the above analysis and computation, we can obtain the following result:

Conclusion 2. System (3) has a supercritical Hopf bifurcation when $r_0 = 0.07716$. If $r < r_0$, the equilibrium becomes unstable, system (3) begins to oscillate.

4. Numerical Examples

In this section, we study the effects of calcium ion flux from outer space through membrane of astrocyte and into cytosol on the dynamics of full system. Regular Ca^{2+} oscillations of the full system as v_{in} increases from $v_{in} = 0.02\,\mu$M/s and $v_{in} = 0.04\,\mu$M/s (blue curve) are plotted in Figure 1. These figures are the result achieved by solving the ordinary differential equations in model of Lavrentovich and Hemkin using Matlab software.

As expected, regular periodic oscillations in cytosolic are generated from numerical simulations. In Figure 1, time evolution of Ca_{cyt} are illustrated for two examples of regular calcium oscillations, that is, a simple spike oscillation with a period of the order of 2000 s at $v_{in} = 0.02\,\mu$M/s (Figure 1(a)), a burst oscillation with a period of the order of 400 s at $v_{in} = 0.04\,\mu$M/s (Figure 1(c)). The corresponding three-dimensional phase portrait diagram in (x, y, z)-plane for $v_{in} = 0.02\,\mu$M/s (Figure 1(b)) and $v_{in} = 0.04\,\mu$M/s (Figure 1(d)) are also plotted, respectively. In Figure 1(c), free calcium ion flux from the outer space into the cytosol caused a large initial peak, which is followed by a small one. In this case, the 3D phase portrait diagram in (x, y, z)-plane is also significantly different.

Based on the stability analysis, we concluded that, in this case, the model has a saddle node for the value of v_{in}. It is seen that the number of peak and the magnitude of each burst increase accordingly, as shown in Figure 2 as $v_{in} = 0.045\,\mu$M/s. Compared to spike oscillation, burst is found to be one of the elementary modes in many cell types, including the neuron and glia. Unlike the case of $v_{in} = 0.04\,\mu$M/s, the free calcium ion current from the outer space into the cytosol caused a large initial peak, which is followed by three small ones, as shown in Figure 2(a). At the same time, the phase portrait diagram in (x, y, z)-plane is rotated at least three times. In order to study the variation of this regular oscillations in detail, two examples of chaotic burst spontaneous Ca^{2+} oscillations are also performed, as shown in Figure 3.

Chaotic oscillation means the system is of total confusion with no order. Figures 1(c), 2(a), 3(a), and 3(c) show the corresponding time series of Ca_{cyt} for two parameter values of $v_{in} = 0.05025\,\mu$M/s and $v_{in} = 0.050252\,\mu$M/s, respectively, for which the number of peak and the magnitude of each burst increase with no order, indicating a state of total confusion. In Figures 3(b) and 3(d), the phase portrait diagram simultaneously exhibits the corresponding attractor, which has been rarely reported in the previous literatures in this astrocyte model. The main difference between the two chaotic burst calcium oscillations is that the order of the chaotic burst oscillation in Figure 3(a) is less than that of the chaotic burst oscillation in Figure 3(c) in both frequency and amplitude.

As the parameter v_{in} increases to $v_{in} = 0.050254\,\mu$M/s, it is observed that each burst comprises two similar spike which means that a small correlation exists between each burst. Compared with the previous finds, in this case, the time evolution and the phase portrait would develop into the long-term depression, as shown in Figures 4(a) and 4(b), respectively. We can predict that as the parameter v_{in} increases further, a simple spike calcium oscillation would occur. To further investigate the generation with respect to the parameter v_{in}, we perform a detailed Hopf bifurcation analysis to the model.

Bifurcation diagram of the whole system with respect to the parameter v_{in} versus Ca_{cyt} (Ca_{er}) is displayed in Figure 5(a) and 5(b). The system begins to oscillate due to a subcritical Hopf bifurcation at point H1 with $v_{in} = 0.01929\,\mu$M/s; meanwhile, a stable limit cycle occurs. With the parameter increasing further, the oscillatory activities terminate and the steady state turns stable again after the parameter $v_{in} = 0.07716\,\mu$M/s at the supercritical Hopf bifurcation point H2. The solid (dashed) curve in Figure 3 denotes the stable (unstable) equilibrium of the steady state. The Matlab software package enables one to simulate the time series and the corresponding phase portrait diagram to verify the effectiveness of our previous prediction.

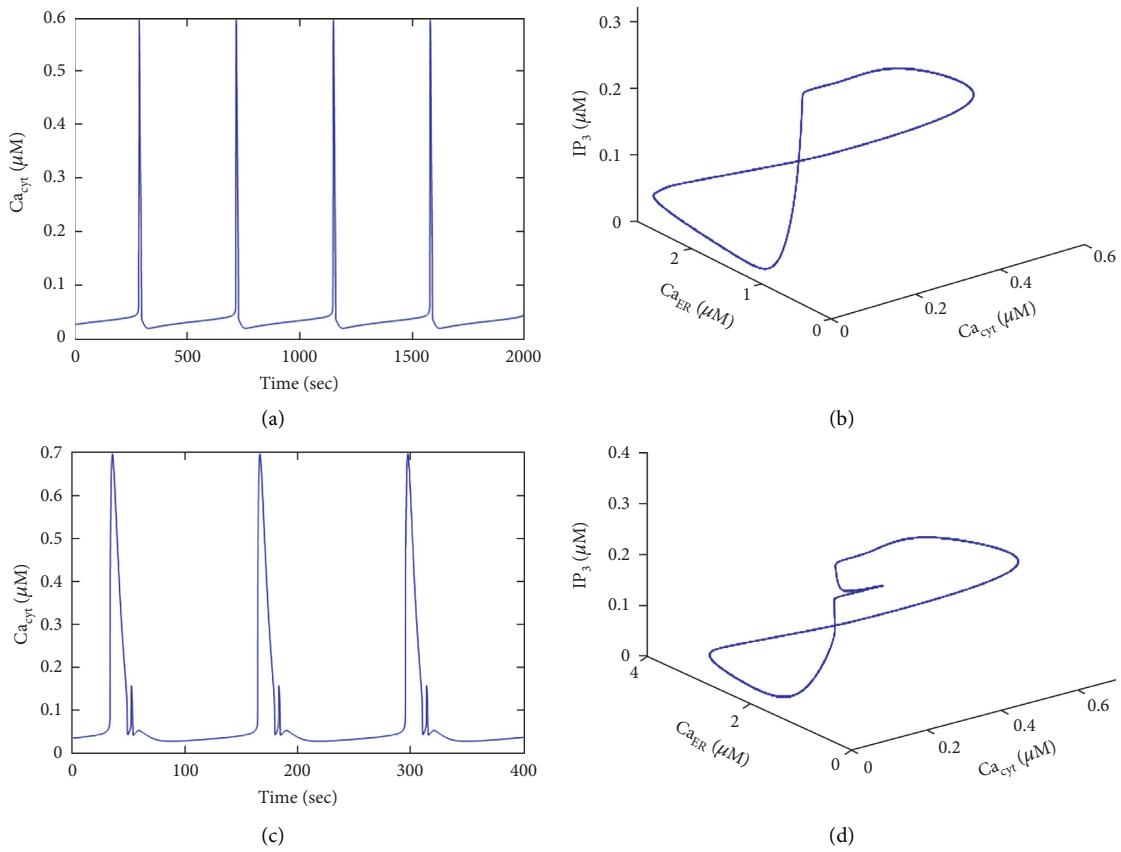

FIGURE 1: Time evolution of regular spontaneous Ca^{2+} oscillations in astrocytes. (a) Simple spike Ca^{2+} oscillations for $v_{in} = 0.02\,\mu$M/s. (b) 3D phase portrait diagram in (x, y, z)-plane for $v_{in} = 0.02\,\mu$M/s. (c) Burst Ca^{2+} oscillations for $v_{in} = 0.04\,\mu$M/s. (d) 3D phase portrait diagram in (x, y, z)-plane for $v_{in} = 0.04\,\mu$M/s.

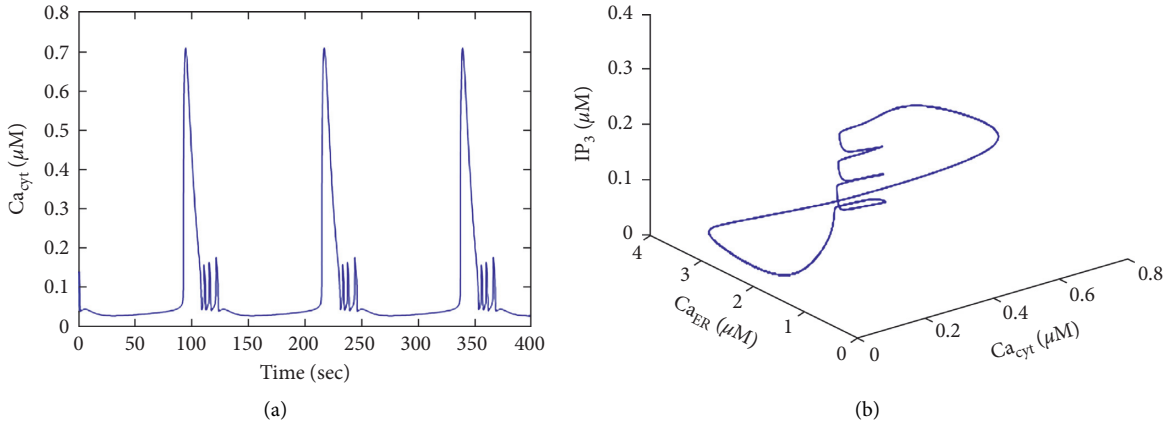

FIGURE 2: Time evolution of regular burst spontaneous Ca^{2+} oscillations in astrocytes. (a) $v_{in} = 0.045\,\mu$M/s. (b) 3D phase portrait diagram in (x, y, z)-plane for $v_{in} = 0.045\,\mu$M/s.

5. Summary

In summary, we have theoretically analyzed a spontaneous Ca^{2+} oscillatory model in astrocyte based on the stability and Hopf bifurcation theory. Firstly, we obtained the sufficient conditions to ensure the model to be stable and the existence of Hopf bifurcation by increasing the parameter v_{in} and the calcium ion current from extracellular space through the membrane of astrocyte and into the cytosol. As v_{in} is slightly more than a critical value, these spontaneous Ca^{2+} oscillations will disappear. Moreover, we concluded that a subcritical Hopf bifurcation point and a supercritical Hopf bifurcation point may be important for the occurrence of spontaneous Ca^{2+} oscillations in astrocytes by applying the

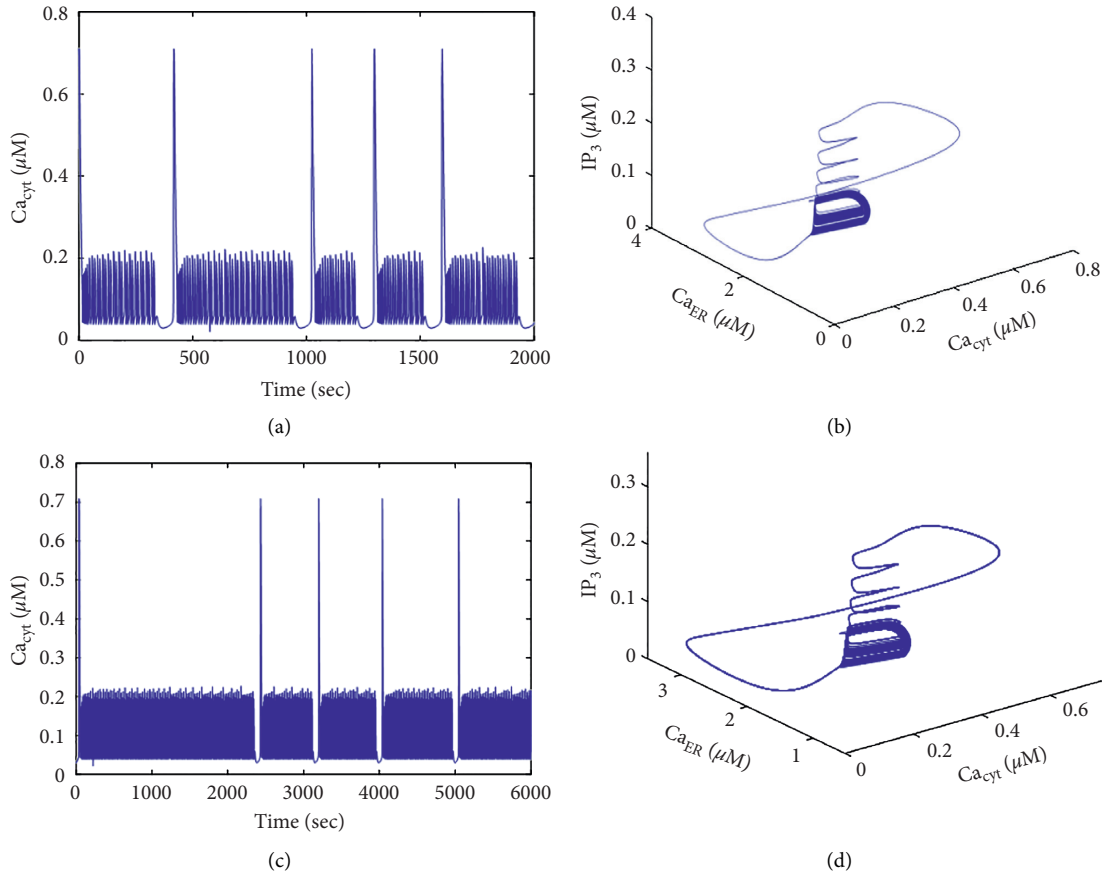

FIGURE 3: Time evolution of chaotic burst spontaneous Ca^{2+} oscillations in astrocytes. (a) $v_{in} = 0.05025\,\mu$M/s. (b) 3D phase portrait diagram in (x, y, z)-plane for $v_{in} = 0.05025\,\mu$M/s. (c)$v_{in} = 0.050252\,\mu$M/s. (d) 3D phase portrait diagram in (x, y, z)-plane for $v_{in} = 0.050252\,\mu$M/s.

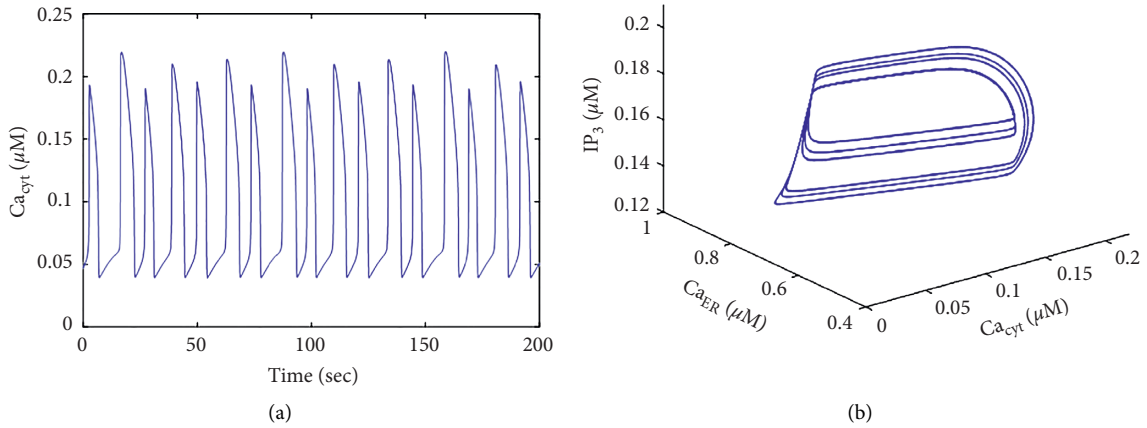

FIGURE 4: Time evolution of regular burst spontaneous Ca2+ oscillations in astrocytes. (a) $v_{in} = 0.050254\,\mu$M/s. (b) 3D phase portrait diagram in (x, y, z)-plane for $v_{in} = 0.050254\,\mu$M/s.

Hopf bifurcation theorem. Moreover, the domain of oscillatory activities with respect to v_{in} is determined by computation using the Hurwitz stability criterion. Finally, based on our theoretical analysis, we give some numerical examples to illustrate the regular and chaotic spontaneous Ca^{2+} oscillations at some certain parameter values. These results demonstrate and enhance our understanding of the generation and transition mechanisms of complex Ca^{2+} oscillations in the astrocyte. These results may be potentially able to better understand the bidirectional signaling pathway between the neuron and glia from a mathematical point of view. Future experimental studies should be undertaken to

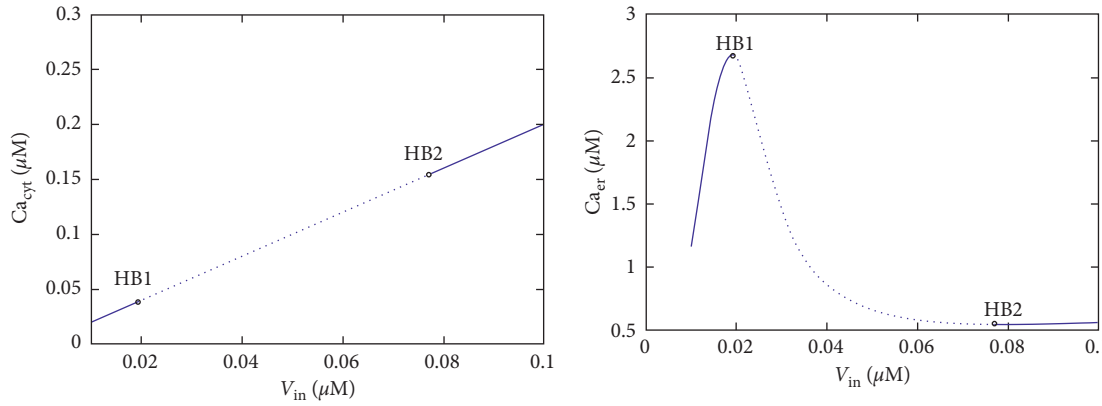

FIGURE 5: (a) Bifurcation diagram of the whole system versus the parameter v_{in} in the (v_{in}, Cacyt)-plane. (b) Bifurcation diagram of the whole system versus the parameter v_{in} in (v_{in}, Caer)-plane. The points HB1 and HB2 represent the subcritical Hopf bifurcation point and the supercritical Hopf bifurcation point, respectively.

discover mechanisms underlying spontaneous Ca^{2+} oscillations in the astrocyte in detail.

Data Availability

All the data utilized in this study have been included within the article, and the sources from where they were adopted were cited accordingly.

Conflicts of Interest

All authors declare no conflicts of interest.

Authors' Contributions

All authors read and approved the last version of the manuscript.

Acknowledgments

This work was supported by the Natural Science Foundation of China under Grant no. 11872084 and Natural Science Foundation of the Anhui Higher Education Institutions of China under Grant nos. KJ2016SD54 and KJ2017A460.

References

[1] M. V. Sofroniew and H. V. Vinters, "Astrocytes: biology and pathology," *Acta Neuropathologica*, vol. 119, no. 1, pp. 7–35, 2010.

[2] B. Reynolds and S. Weiss, "Generation of neurons and astrocytes from isolated cells of the adult mammalian central nervous system," *Science*, vol. 255, no. 5052, pp. 1707–1710, 1992.

[3] N. J. Abbott, L. Rönnbäck, and E. Hansson, "Astrocyte-endothelial interactions at the blood-brain barrier," *Nature Reviews Neuroscience*, vol. 7, no. 1, pp. 41–53, 2006.

[4] J. W. Fawcett and R. A. Asher, "The glial scar and central nervous system repair," *Brain Research Bulletin*, vol. 49, no. 6, pp. 377–391, 1999.

[5] V. Parpura, T. A. Basarsky, F. Liu, K. Jeftinija, S. Jeftinija, and P. G. Haydon, "Glutamate-mediated astrocyte-neuron signalling," *Nature*, vol. 369, no. 6483, pp. 744–747, 1994.

[6] E. A. Newman and K. R. Zahs, "Modulation of neuronal activity by glial cells in the retina," *The Journal of Neuroscience*, vol. 18, no. 11, pp. 4022–4028, 1998.

[7] A. Cornell-Bell, S. Finkbeiner, M. Cooper, and S. Smith, "Glutamate induces calcium waves in cultured astrocytes: long-range glial signaling," *Science*, vol. 247, no. 4941, pp. 470–473, 1990.

[8] V. V. Matrosov and V. B. Kazantsev, "Bifurcation mechanisms of regular and chaotic network signaling in brain astrocytes," *Chaos: an Interdisciplinary Journal of Nonlinear Science*, vol. 21, no. 2, Article ID 023103, 2011.

[9] M. V. Sofroniew, "Molecular dissection of reactive astrogliosis and glial scar formation," *Trends in Neurosciences*, vol. 32, no. 12, pp. 638–647, 2009.

[10] M. Pekny and M. Nilsson, "Astrocyte activation and reactive gliosis," *Glia*, vol. 50, no. 4, pp. 427–434, 2005.

[11] M. Zonta, M. C. Angulo, S. Gobbo et al., "Neuron-to-astrocyte signaling is central to the dynamic control of brain microcirculation," *Nature Neuroscience*, vol. 6, no. 1, pp. 43–50, 2003.

[12] D. E. Postnov, R. N. Koreshkov, N. A. Brazhe, A. R. Brazhe, and O. V. Sosnovtseva, "Dynamical patterns of calcium signaling in a functional model of neuron-astrocyte networks," *Journal of Biological Physics*, vol. 35, no. 4, pp. 425–445, 2009.

[13] J. J. Wade, L. J. McDaid, J. Harkin, V. Crunelli, and J. A. Kelso, "Bidirectional coupling between astrocytes and neurons mediates learning and dynamic coordination in the brain: a multiple modeling approach," *PLoS One*, vol. 6, no. 12, Article ID e29445, 2011.

[14] G. Karimi, M. Ranjbar, M. Amirian, and A. Shahim-aeen, "A neuromorphic real-time VLSI design of Ca2+ dynamic in an astrocyte," *Neurocomputing*, vol. 272, no. 10, pp. 197–203, 2018.

[15] S. Mederos, C. Gonzalezarias, G. Perea et al., "Astrocyte-neuron networks: a multilane highway of signaling for homeostatic brain function," *Frontiers in Synaptic Neuroscience*, vol. 6, p. 32343, 2018.

[16] B. Ermentrout, *Simulating, Analyzing, and Animating Dynamical Systems: A Guide to XPPAUT for Researchers and*

Students, Society for Industrial and Applied Mathematics, Philadelphia, PA, USA, 2002.

[17] Y. A. Kuznetsov and V. V. Levitin, *CONTENT: A Multiplatform Environment for Analyzing Dynamical Systems*, Dynamical Systems Laboratory, Amsterdam, The Netherlands, 1997.

[18] Y.-X. Li and J. Rinzel, "Equations for InsP3 receptor-mediated [Ca2+]i oscillations derived from a detailed kinetic model: a hodgkin-huxley like formalism," *Journal of Theoretical Biology*, vol. 166, no. 4, pp. 461–473, 1994.

[19] Q. Ji and Y. Lu, "Bifurcations and continuous transitions in a nonlinear model of intracellular calcium oscillations," *International Journal of Bifurcation and Chaos*, vol. 23, no. 02, p. 1350033, 2013.

[20] Q. Ji, Y. Zhou, Z. Yang, and X. Meng, "Evaluation of bifurcation phenomena in a modified shen-larter model for intracellular $$\hbox {Ca}^{\varvec{2+}}$$ Ca^{2+} bursting oscillations," *Nonlinear Dynamics*, vol. 84, no. 3, pp. 1281–1288, 2016.

[21] F. Oschmann, H. Berry, K. Obermayer, and K. Lenk, "From in silico astrocyte cell models to neuron-astrocyte network models: a review," *Brain Research Bulletin*, vol. 136, pp. 76–84, 2018.

[22] V. Matrosov, S. Gordleeva, N. Boldyreva, E. Ben-Jacob, V. Kazantsev, and M. De Pittà, "Emergence of regular and complex calcium oscillations by inositol 1, 4, 5-trisphosphate signaling in astrocytes," *Springer Series in Computational Neuroscience*, vol. 2019, pp. 151–176, 2019.

[23] M. Enomoto and S. Kawazu, "Blockage of spontaneous Ca^{2+} oscillation causes cell death in intraerythrocytic Plasmodium falciparum," *PLoS One*, vol. 7, no. 7, Article ID e39499, 2012.

[24] M. Zonta and G. Carmignoto, "Calcium oscillations encoding neuron-to-astrocyte communication," *Journal Physiology-Paris*, vol. 96, no. 3-4, pp. 193–198, 2002.

[25] S. Zeng, B. Li, S. Zeng, and S. Chen, "Simulation of spontaneous Ca2+ oscillations in astrocytes mediated by voltage-gated calcium channels," *Biophysical Journal*, vol. 97, no. 9, pp. 2429–2437, 2009.

[26] C. Agulhon, T. A. Fiacco, and K. D. McCarthy, "Hippocampal short- and long-term plasticity are not modulated by astrocyte Ca2+ signaling," *Science*, vol. 327, no. 5970, pp. 1250–1254, 2010.

[27] Y. Otsu, K. Couchman, D. G. Lyons et al., "Calcium dynamics in astrocyte processes during neurovascular coupling," *Nature Neuroscience*, vol. 18, no. 2, pp. 210–218, 2015.

[28] M. Naeem, L. J. McDaid, J. Harkin, J. J. Wade, and J. Marsland, "On the role of astroglial syncytia in self-repairing spiking neural networks," *IEEE Transactions on Neural Networks and Learning Systems*, vol. 26, no. 10, pp. 2370–2380, 2015.

[29] M. Lavrentovich and S. Hemkin, "A mathematical model of spontaneous calcium (II) oscillations in astrocytes," *Journal of Theoretical Biology*, vol. 251, no. 4, pp. 553–560, 2008.

[30] B. Chander and V. Chakravarthy, "A computational model of neuro-glio-vascular loop interactions," *PLoS ONE*, vol. 7, Article ID e48802, 2012.

[31] J. Li, J. Tang, J. Ma, M. Du, R. Wang, and Y. Wu, "Dynamic transition of neuronal firing induced by abnormal astrocytic glutamate oscillation," *Scientific Reports*, vol. 6, Article ID 32343, 2016.

[32] J. Li, Y. Xie, Y. Yu, M. Du, R. Wang, and Y. Wu, "A neglected GABAergic astrocyte: calcium dynamics and involvement in seizure activity," *Science China Technological Sciences*, vol. 60, no. 7, pp. 1003–1010, 2017.

[33] T. Manninen, R. Havela, M. Linne et al., "Computational models for calcium-mediated astrocyte functions," *Frontiers in Computational Neuroscience*, vol. 201814 pages, 2018.

[34] H. Wang, Q. Wang, and Q. Lu, "Bursting oscillations, bifurcation and synchronization in neuronal systems," *Chaos, Solitons & Fractals*, vol. 44, no. 8, pp. 667–675, 2011.